Extracellular vesicles as drug delivery systems for protein replacement therapeutics in rare diseases

Dr Simó Schwartz Jr

Barcelona Vall d'Hebron Hospital Campus

Vall d'Hebron Institut de Recerca (VHIR)

25th March 2022, Barcelona

Extracellular vesicles (EV)

Highly heterogeneous in size, composition, origin and function

Main role acknowledge: Intercellular communication

Microvesicles, ectosomes, shedding vesicles **- EV in the µmetric scale 150-1000nm**

Exosomes – EV in the nanometric scale 30-100nm

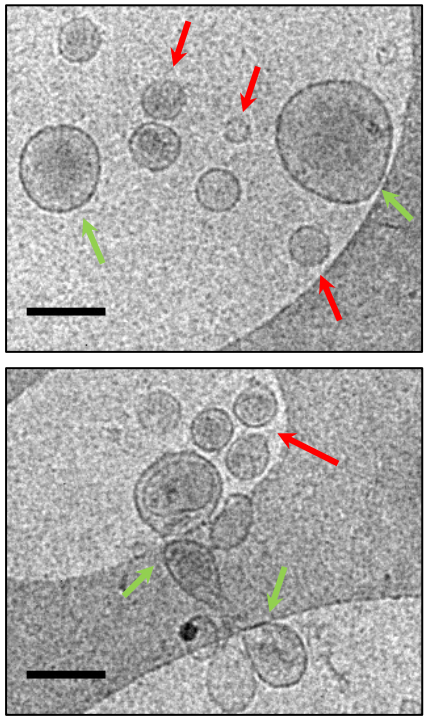

EV from CHO GLA-CMYC-H6 producing cells. Scale bar 200 nm.

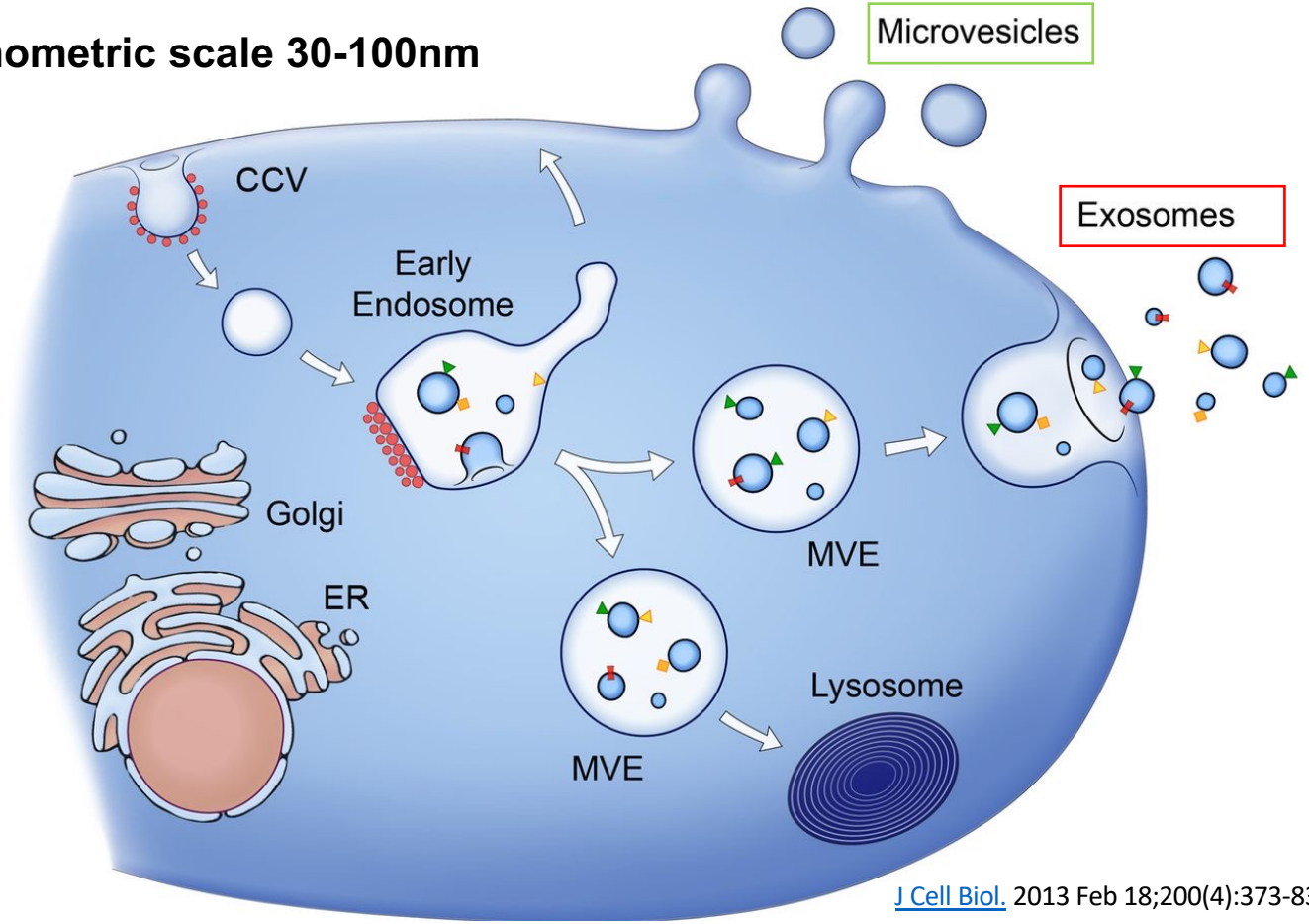

J Cell Biol. 2013 Feb 18;200(4):373-83.

EV/ Exosome as Drug Delivery Systems (DDS)

1. **Biocompatible and biodegradable**
2. **Low toxicity and immunogenicity**
3. **Easily generated (most cell types can produce exosomes)**
4. **Stable in biological fluids**
5. **Can be engineered for precise drug and therapeutic nucleic acid delivery.**
   a) **Genetically modified – Bottom up approach**
   b) **Mechanically/Chemically loaded – Top down approach**

Table 1. Examples of engineering exosomes for cargo delivery.

		Advantages	Disadvantages	Model drugs
I) Passive loading	a) Incubation of exosomes and free drugs	Simple Do not compromise membrane integrity	Low drug loading efficiency	Doxorubicin[60] Paclitaxel[48] Catalase[44] Paclitaxel[58]
	b) Incubation of the donor cells with free drugs	Simple Do not compromise membrane integrity	Low drug loading efficiency Drugs may cause cytotoxicity to the donor cells	
II) Active loading	a) Sonication	High drug loading efficiency	Compromise membrane integrity	Catalase[44]
	b) Extrusion	High drug loading efficiency	Compromise membrane integrity	Porphyrin[50]
	c) Freeze/thaw	Medium drug loading efficiency Liposome-exosome fusion	Aggregations	Porphyrin
	d) Electroporation	Loading with large molecules such as siRNA, miRNA	Aggregations	let-7a miRNA[66] MAPK1 siRNA[52]
	e) Incubation with saponin	Enhanced drug loading	Toxicity	Catalase[44] Porphyrin[50]
	f) Click chemistry	Quick and efficient Better control over the conjugation site		Azide-fluor 545 for *in vitro* tracking[56]
	g) Antibody binding	Specific and easy to operate		CD9 antibody with Alexa-647[57]

Acta Pharmacol Sin. 2017 Jun;38(6):754-763.doi: 10.1038/aps.2017.12

EV/Exosomes

To generate and EV-based DDS.

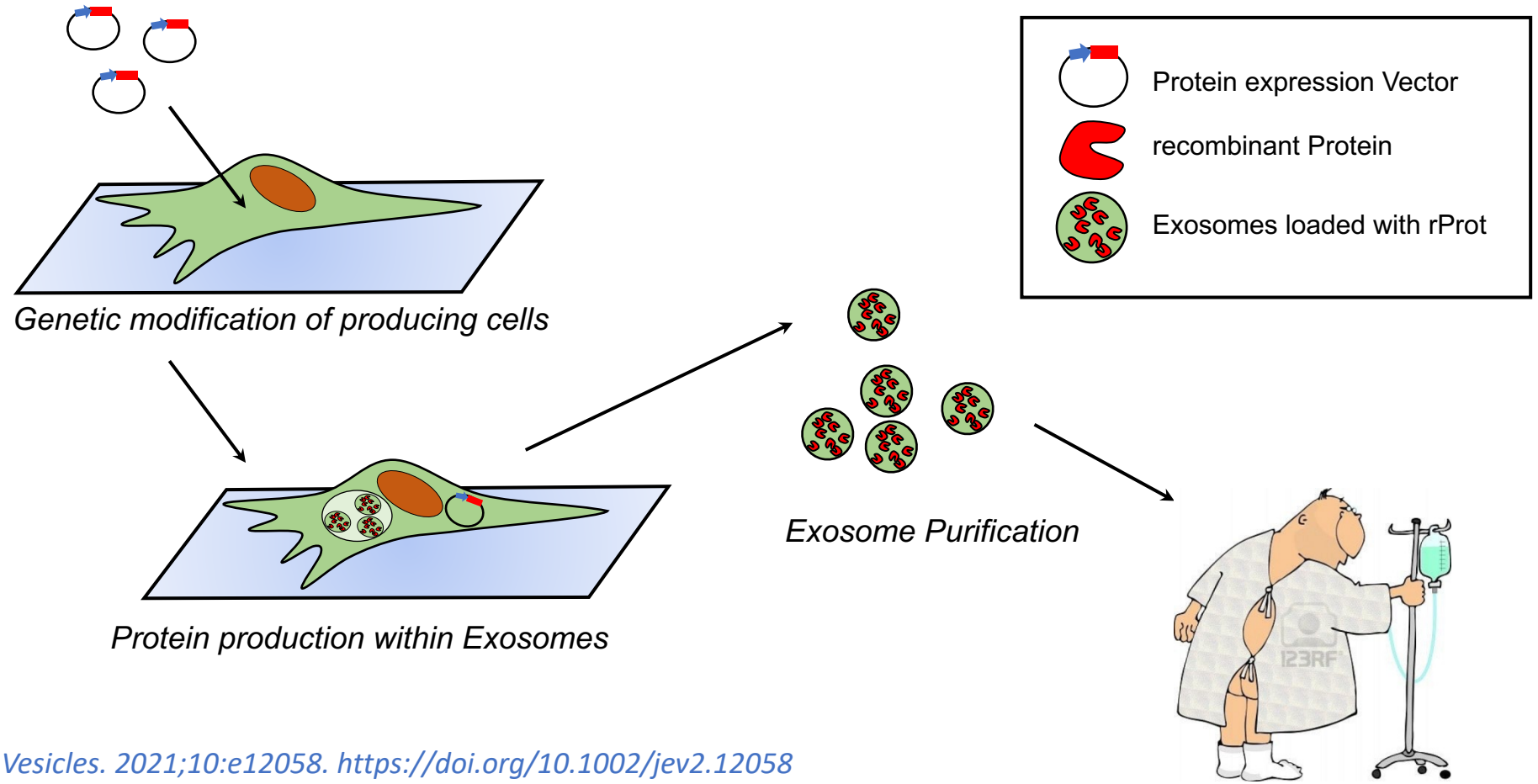

J Extracell Vesicles. 2021;10:e12058. https://doi.org/10.1002/jev2.12058

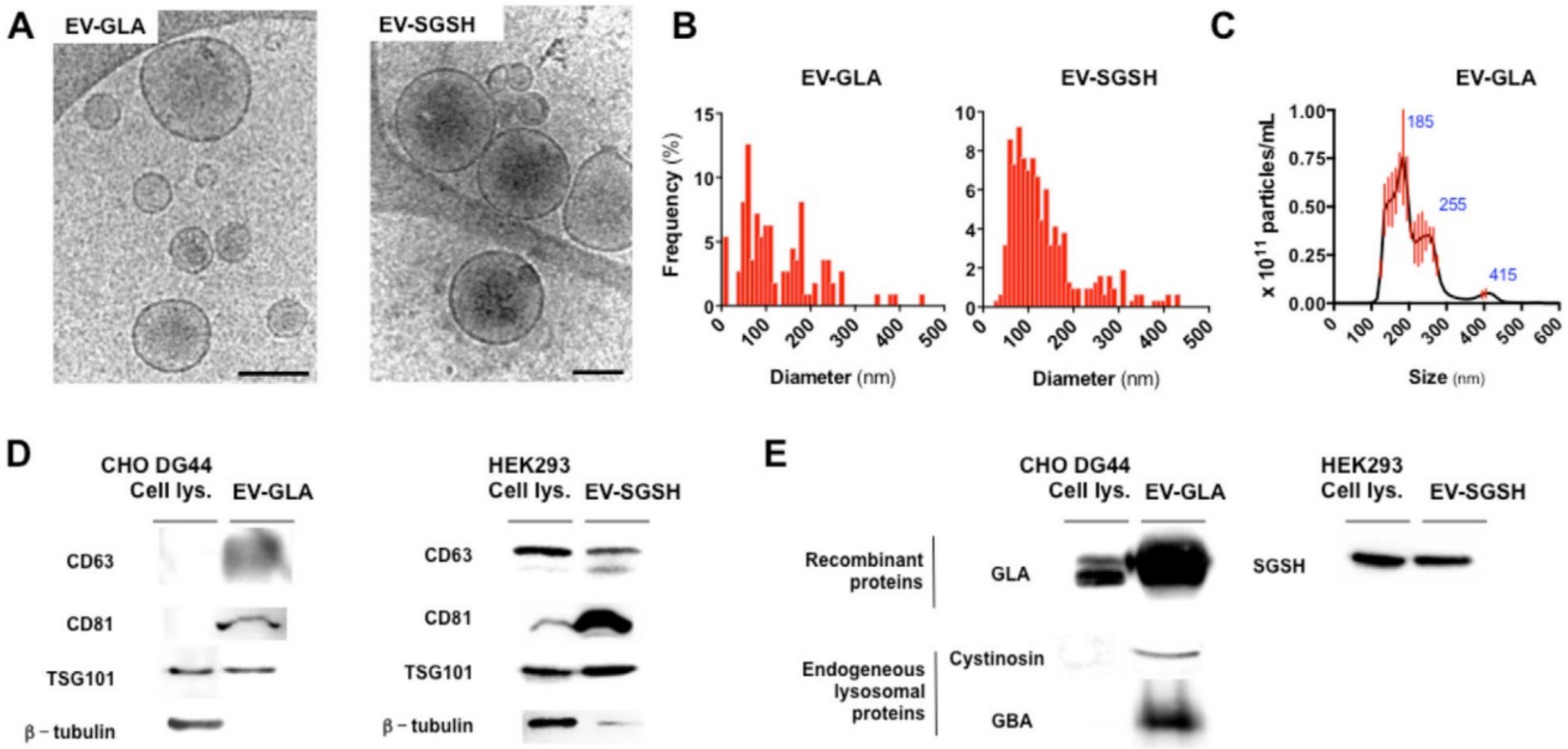

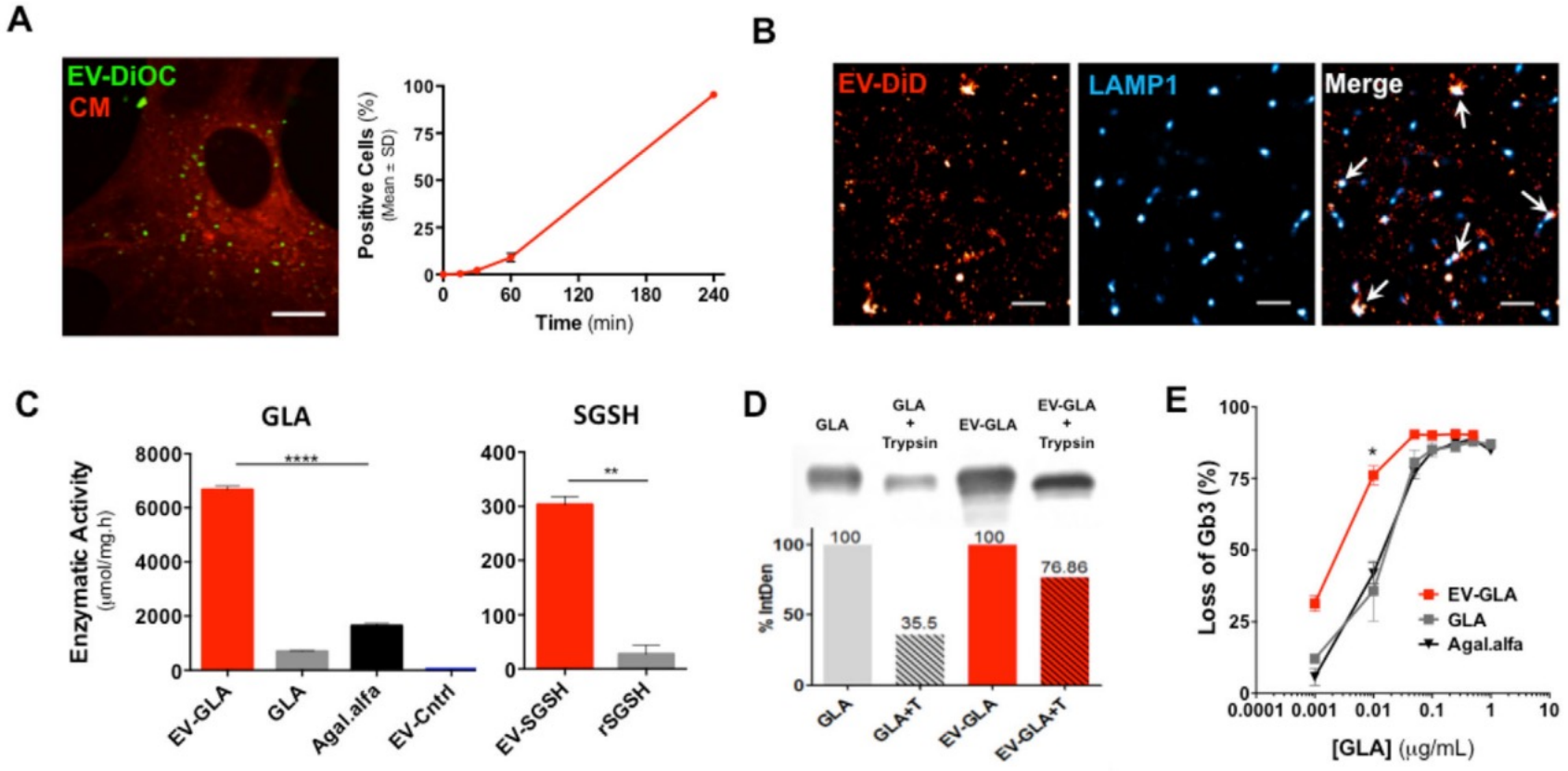

FIGURE 2 In vitro assessment of EVs as drug delivery systems for lysosomal proteins. **A)** Internalization of EVs by confocal microscopy (4 h incubation) and flow cytometry in primary cultures of mouse aortic endothelial cells (MAEC) derived from Fabry KO mice. EVs were labelled with DiOC (green) and cell membranes were labelled with Cell Mask (red). Magnification bar corresponds to 10 μm. **B)** Inset of HEK293 cytoplasmatic region of a single cell showing colocalization (white arrows) of EV-GLA labelled with DiD (red) with lysosomal marker LAMP1 (blue) by STORM imaging. Magnification bar corresponds to 1 μm. **C)** Enzymatic activities for alpha-galactosidase A (left) and heparan sulfatase (right) measured in EVs obtained from cells overexpressing GLA and SGSH proteins, respectively. EVs from non-transfected CHO cells were also included as controls (EV-Control). **D)** Protease digestion assay of EV-GLA (red bars) and their naked GLA counterparts (grey bars). T stands for trypsin treatment. %IntDen refers to the percentage of the integrated density. **E)** Efficacy of EV-GLA reducing the Gb3 deposits in MAEC primary cultures at different GLA protein concentrations

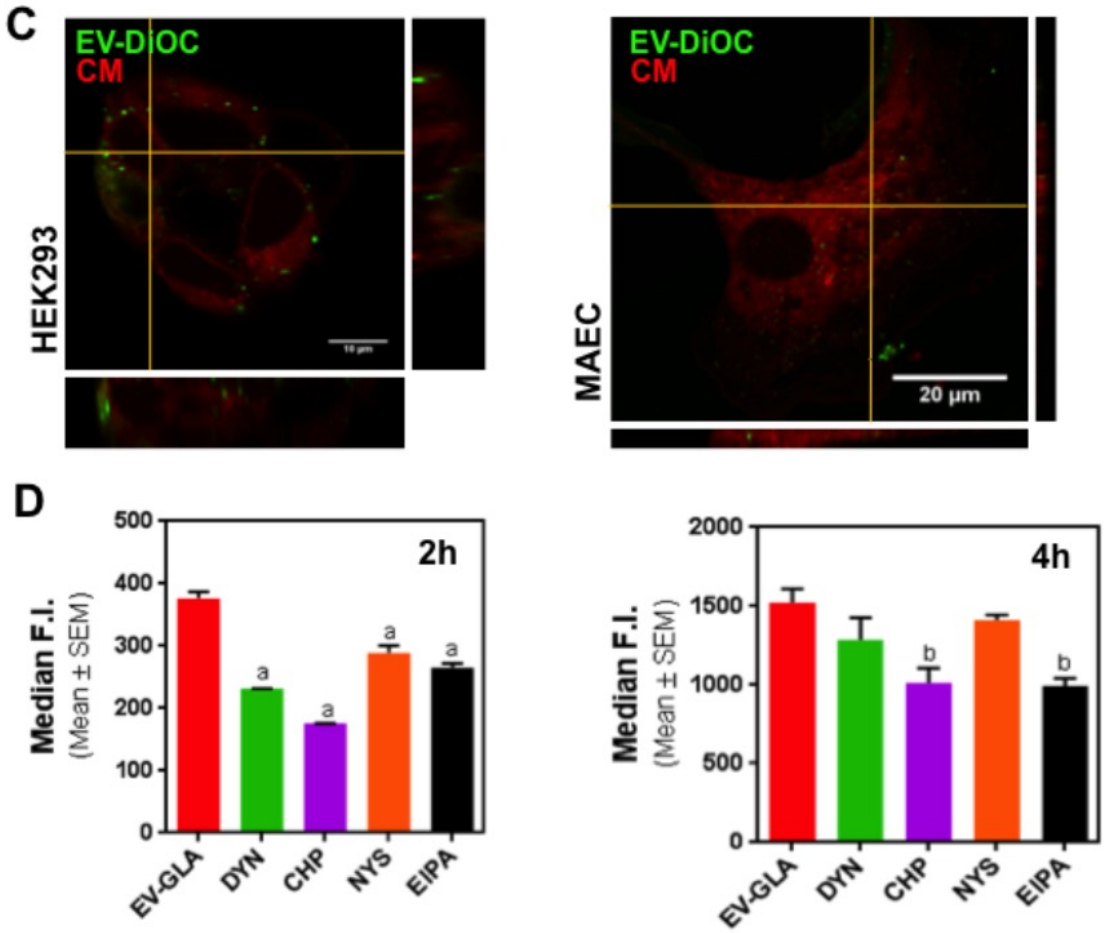

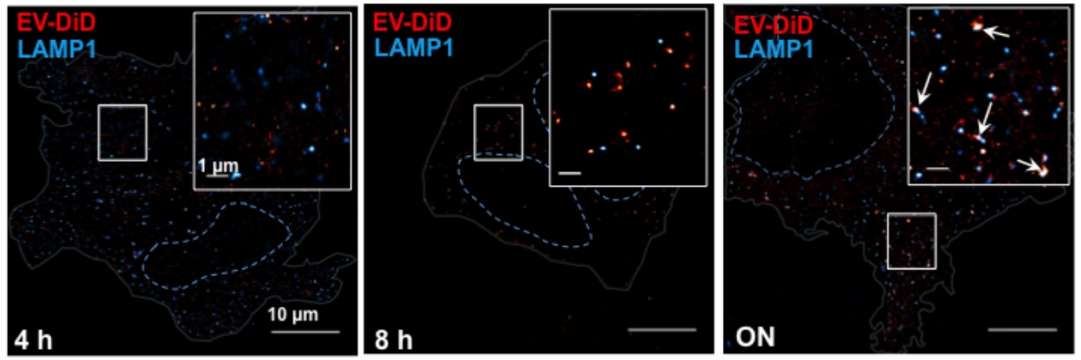

Figure S4. STORM images of EV colocalization with LAMP1 lysosomal marker. HEK293 cells after 4 h, 8 h and ON incubation with DiD-labeled EV-GLA. Nuclei in each cell are outlined with a blue dashed line. Insets show a cytoplasmatic region for further detail of EV-GLA and LAMP1 interaction.

Inhibitors legend: dynasore (DYN) 80 μM –inhibition of endocytic vesicle scission from cell membrane–, chlorpromazine (CHP) 20 μM –inhibition of clathrin mediated endocytosis–, nystatin (NYS) 50 μM –inhibition of caveolae mediated endocytosis– and 5-(N-ethyl-N-isopropyl) amiloride (EIPA) 100 μM –inhibition of macropynocitosis–

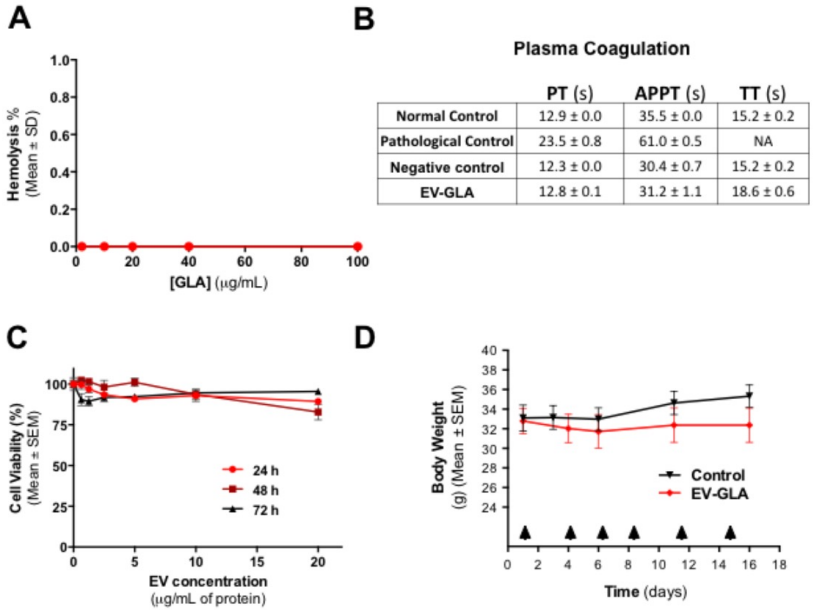

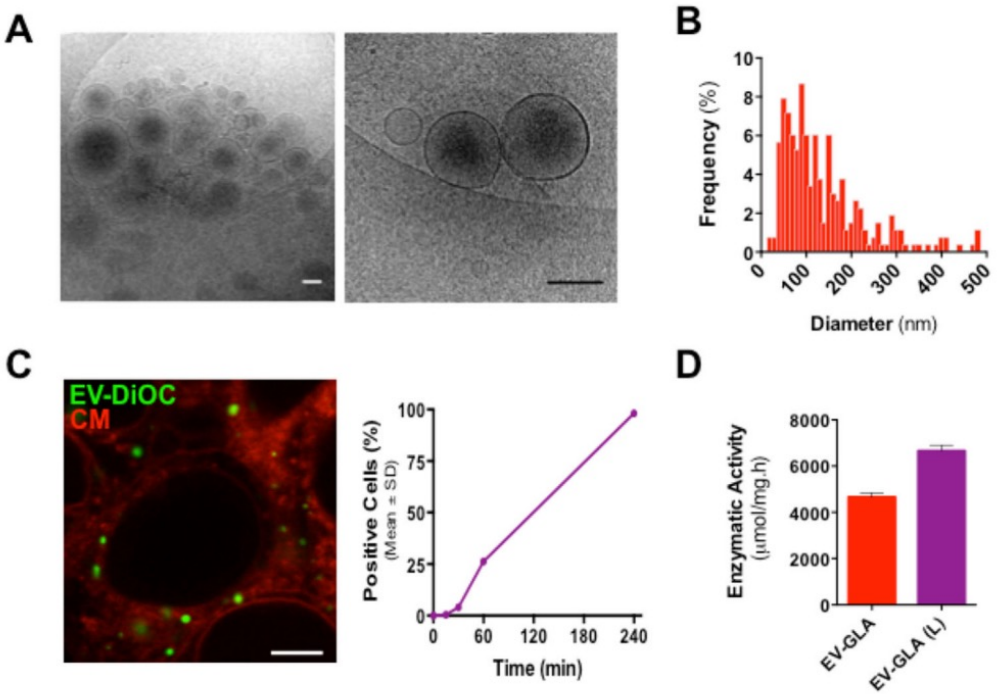

FIGURE 3 EVs stability after lyophilization. **A)** CryoTEM images of EV-GLA after lyophilization. Magnification bars correspond to 200 nm. **B)** Size distribution of EV-GLA post-lyophilization. **C)** Cell internalization of lyophilized EV by confocal microscopy (left panel) and flow cytometry (right panel) in HEK293 cells. For microscope imaging, EVs were labelled with DiOC (green) and cell membranes stained with Cell Mask (CM, red). DiD-labelled EV-GLA were used for cell cytometry. Magnification bar corresponds to 5 μm. **D)** Specific enzymatic activity of GLA in EVs before (red bar) and after lyophilization (purple bar)

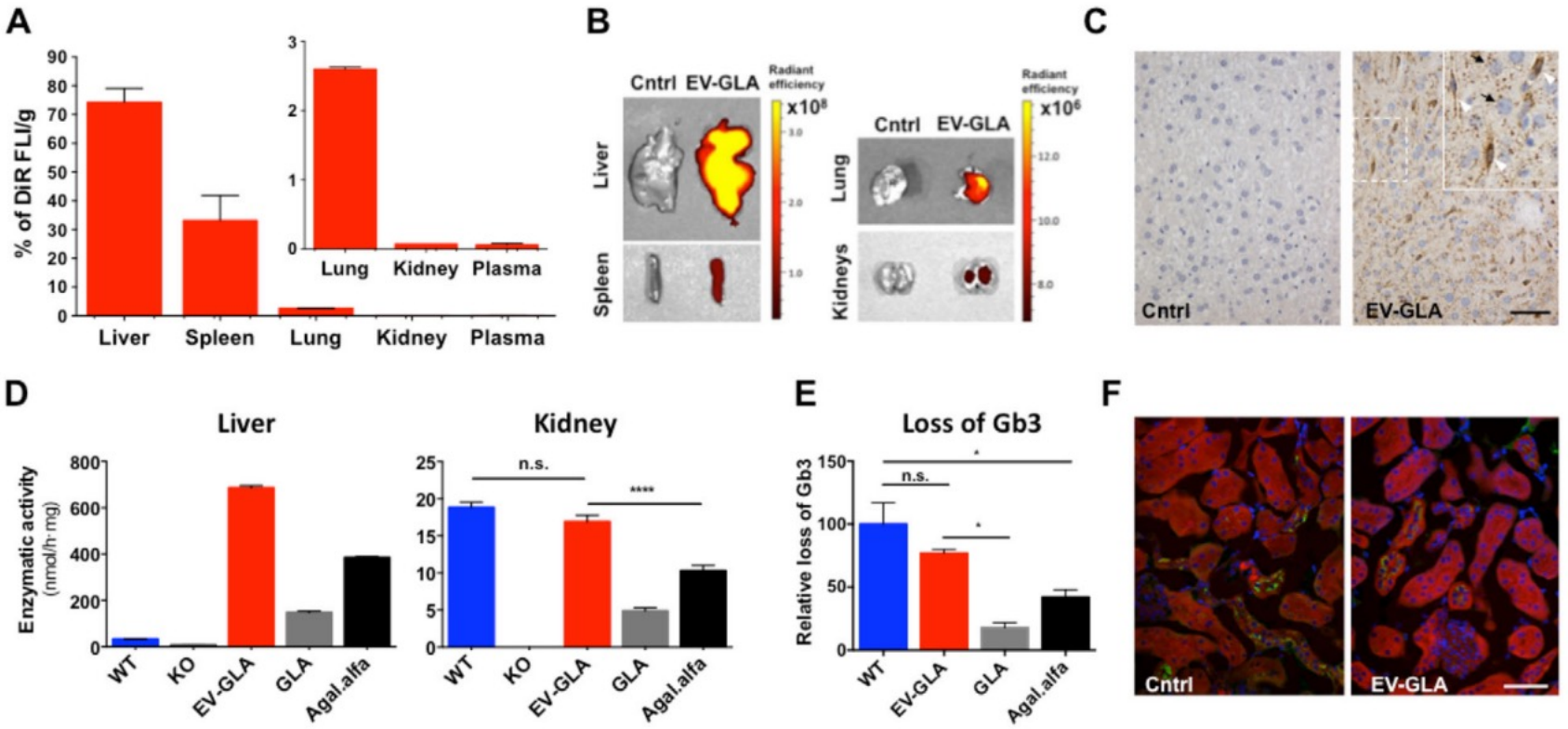

FIGURE 4 In vivo biodistribution and single-dose efficacy of EV-GLA in Fabry KO mice. **A)** Biodistribution of DiR-labelled EVs in Fabry KO mice 1 h after i.v. administration (100 μg of protein) showed a widespread distribution of the fluorescent signal in different organs. **B)** Ex vivo fluorescence images of the liver and kidneys. **C)** GLA protein detected by immunohistochemistry in liver tissues of GLA KO mice administered with vehicle (Cntrl) or EV-GLA. Magnification bar corresponds to 50 μm. Inset contains a magnified area to identify hepatocytes (black arrows) and Kupffer cells (withe arrowheads) (**D)** GLA enzymatic activity measurements of mice treated with a single administration of EV-GLA, free enzyme GLA or agalsidase alfa at 1 mg GLA/kg and euthanized 1 h post-administration in liver and kidneys. WT animals and non-treated KO animals were also included in the assay. **E)** Loss of Gb3 in KO mice treated with a single dose of EV-GLA, free enzyme GLA or agalsidase alfa (1 mg/kg) and euthanized 1 week after. **F)** Immunofluorescence of Gb3 (green signal) in kidneys of KO animals, vehicle-treated (Cntrl) or receiving one i.v. dose of EV-GLA (1 mg/kg). Nuclei were stained with DAPI (blue) and cells with rhodamine-phalloidin (red). Magnification bar corresponds to 40 μm

EVs –GLA efficacy in vivo

Gb3 clearance detected by MS

J Extracell Vesicles. 2021;10:e12058. https://doi.org/10.1002/jev2.12058

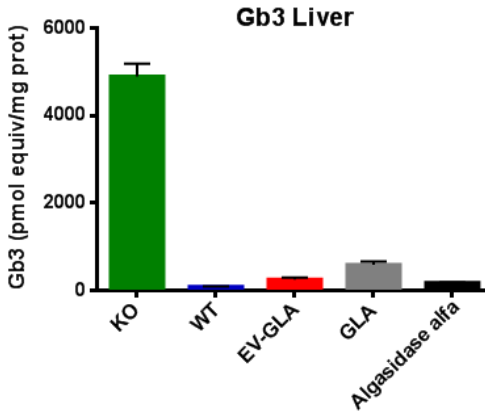

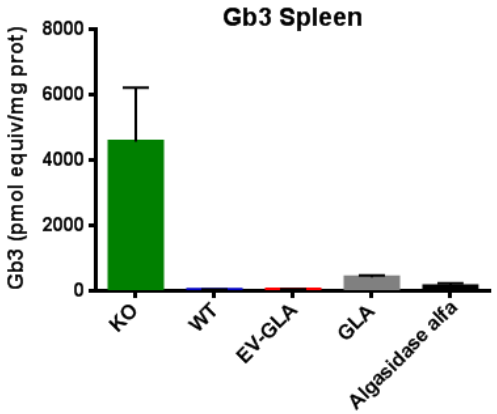

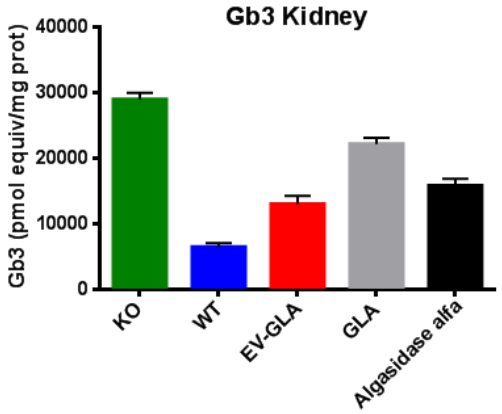

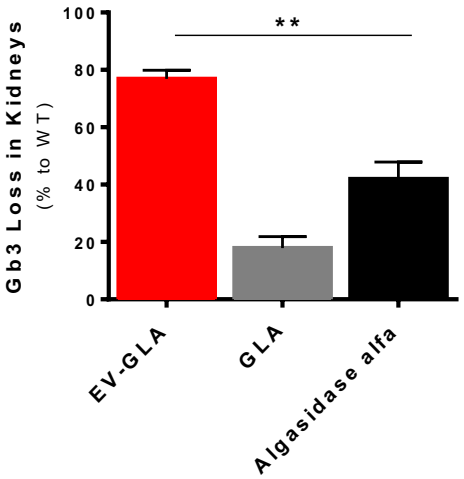

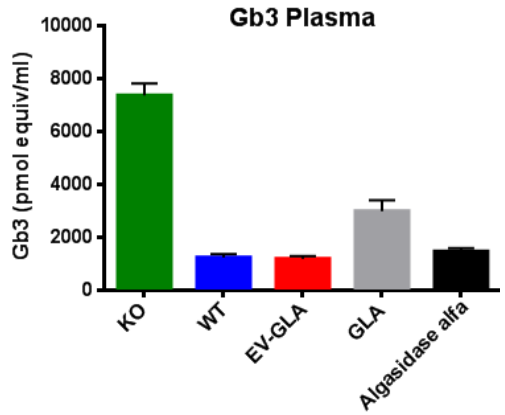

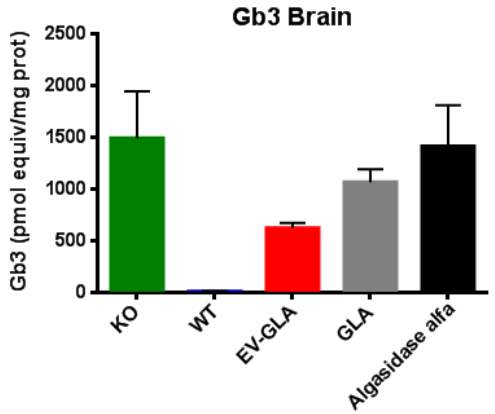

Marked **decrease of Gb3 in all the organs** tested for EV-GLA.

In kidney EV-GLA is also significantly **more effective than the Aglasidase alfa**.

Unexpectedly EV-GLA showed efficacy in brain indicating a **BBB crossing** of the EV-GLA.

Enzymatic activity in the kidney

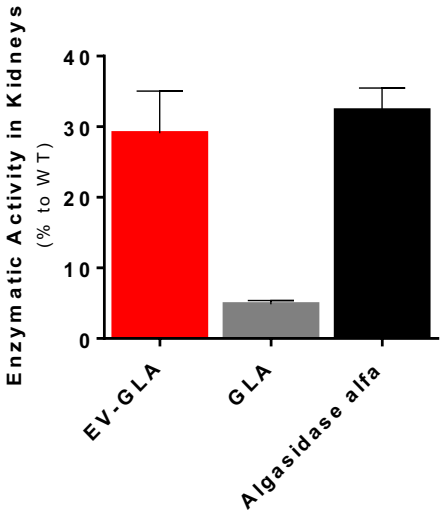

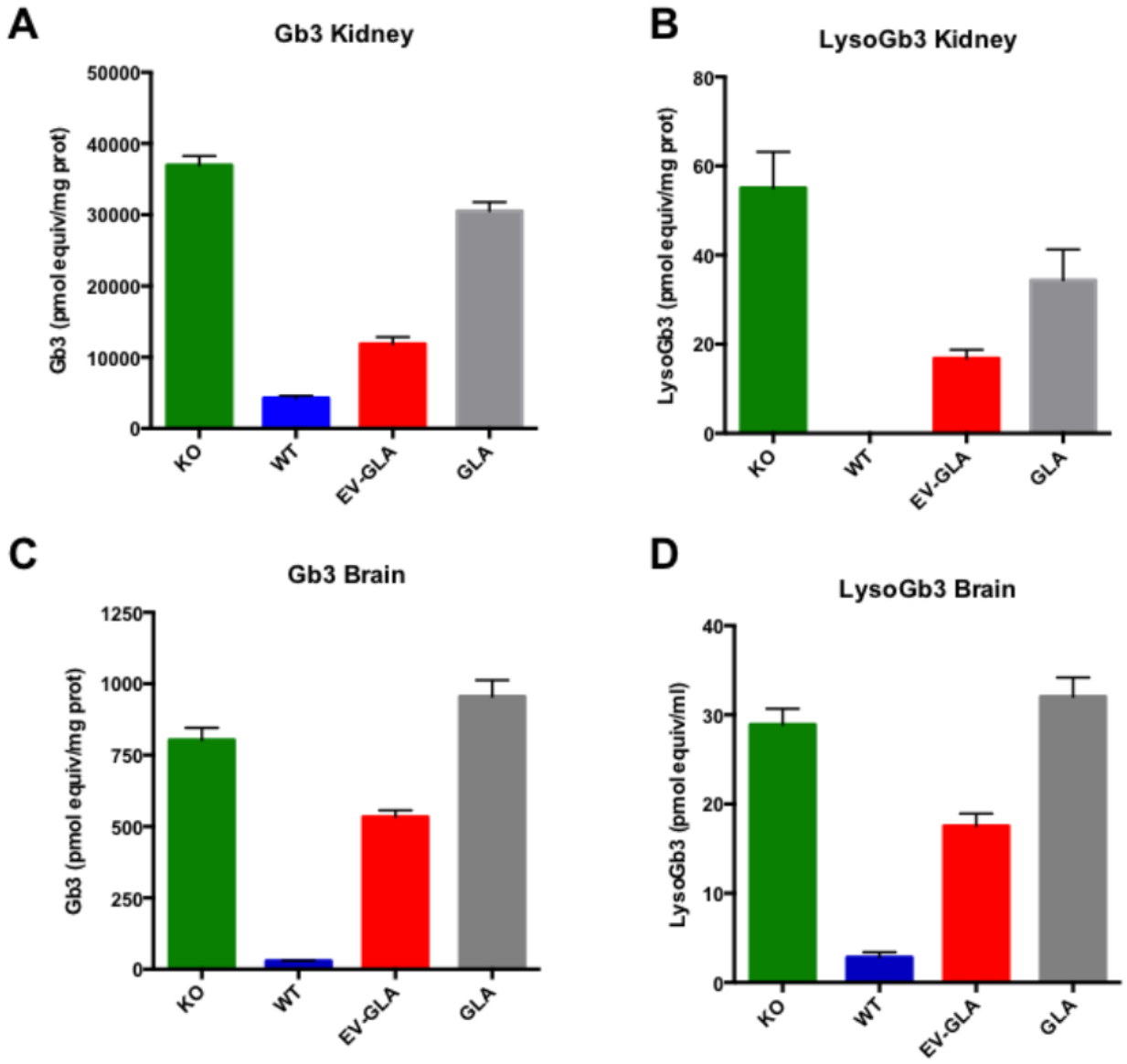

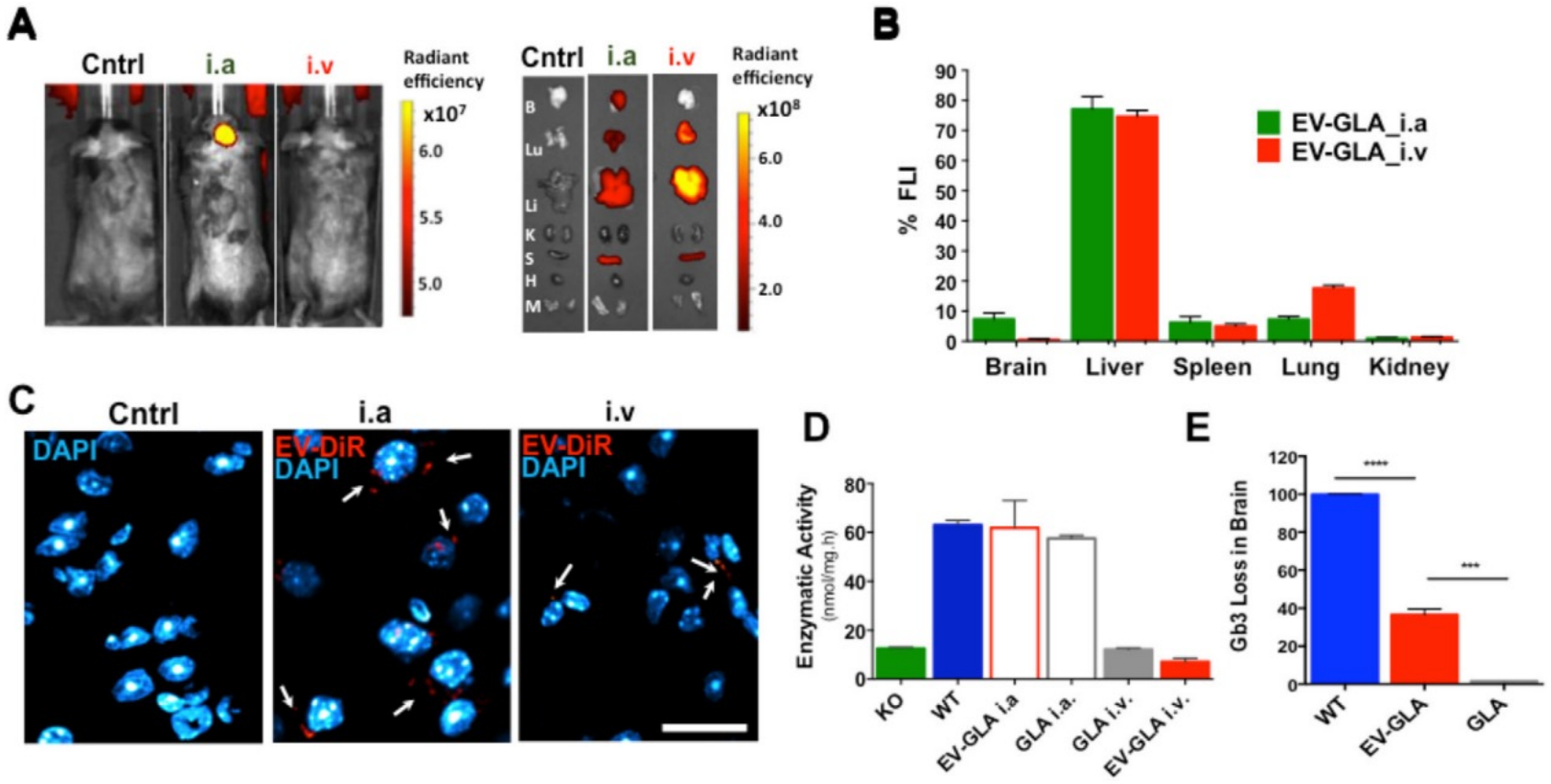

FIGURE 5 EV-GLA in the brain parenchyma. **A)** In vivo (left panel) and ex vivo (right panel) fluorescence imaging (FLI) of Fabry KO mice receiving either intra-arterial (i.a.) or intravenous (i.v.) administration of DiR-labelled EV-GLA (1 mg/kg of GLA) compared to the non-treated controls (Cntrl). Ex vivo imaging included brain (B), lungs (Lu), liver (Li), kidneys (K), spleen (S), heart (H) and muscle (M). **B)** FLI signal quantification comparing biodistribution of EV-GLA after i.v. or i.a. administration. **C)** Confocal images of brain parenchyma showing DiR fluorescent signal of EV-GLA (red) and DAPI-labelled cell nuclei (blue). Magnification bar corresponds to 20 μm. **D)** GLA enzymatic activity 1 h post-administration in brains of Fabry KO mice treated with GLA or EV-GLA via i.v. or i.a. administrations **E)** Loss of Gb3 in KO mice treated i.v. with a single dose of EV-GLA, as measured by LC-HRMS 1 week after dosing

EVs –Non Lysosomal protein delivery – angiogenic proteins

Control -

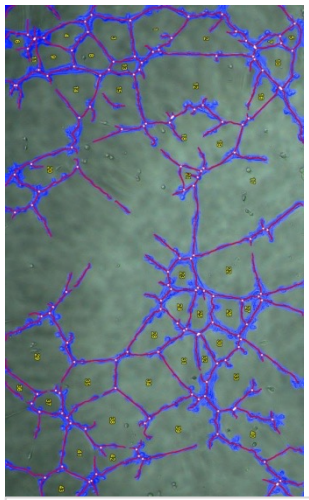

EVs- Angio

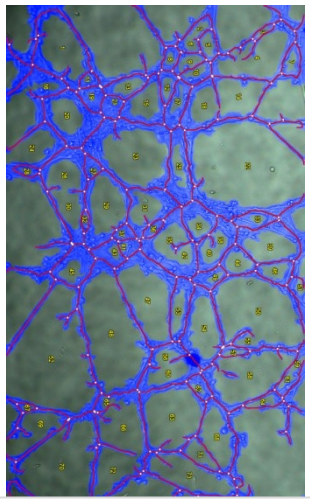

Control + (rAngio)

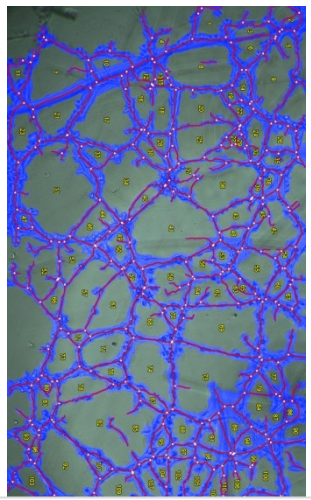

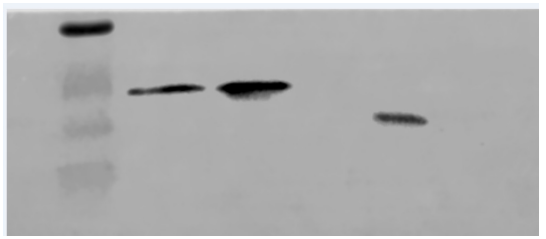

Angiogenin detection - WB

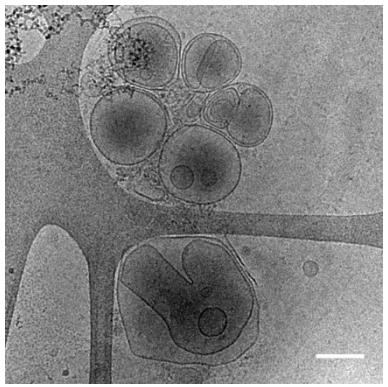

EVs-Angio 200 nm

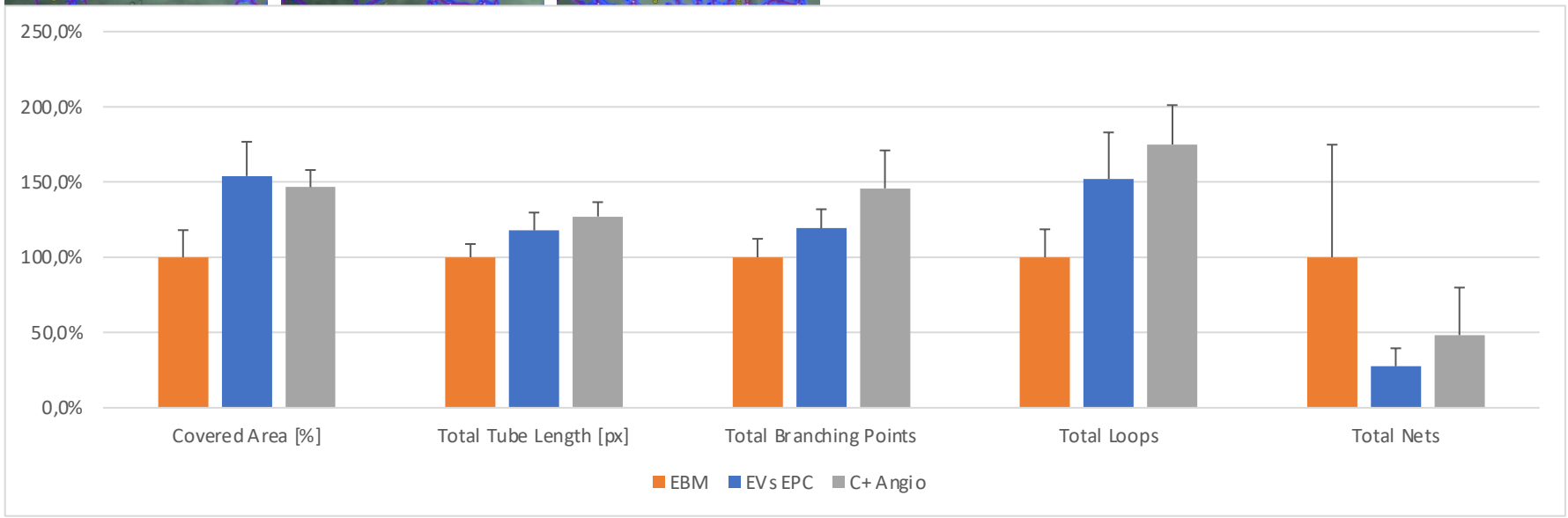

Vall d'Hebron Hospital CIBBIM - Nanomedicina

Vall d'Hebron Barcelona Hospital Campus

Vall d'Hebron Hospital

Vall d'Hebron Institut de Recerca

VHIO Vall d'Hebron Institute of Oncology

Cemcat

ciber-bbn

nanbiosis

COST ACTION CA 17140 NANO2CLINIC CANCER NANOMEDICINE - FROM THE BENCH TO THE BEDSIDE

cost EUROPEAN COOPERATION IN SCIENCE & TECHNOLOGY

Vall d'Hebron
Hospital
CIBBIM - Nanomedicina

CIBBIM-Nanomedicine

Drug Delivery and Targeting

Simo Schwartz Jr

Ibane Abasolo (PhD)

Fernanda Andrade (PhD)

Patricia González Cámara (PhD)

Diana Rafael Fernandes (PhD)

Petra Gener (PhD)

Joaquin-Seras Franzoso (PhD)

Vanessa Diaz-Riascos (PhD)

Francesc Martinez Trucharte (MsC)

Vall d'Hebron
Hospital
CIBBIM - Nanomedicina